Nuclear Instruments and Methods in Physics Research A 664 (2012) 154–160

Contents lists available at SciVerse ScienceDirect

Nuclear Instruments and Methods in Physics Research A

journal homepage: www.elsevier.com/locate/nima

Calibration factors for determination of relativistic particle induced fission rates in ^{nat}U, ^{235}U, ^{232}Th, ^{nat}Pb and ^{197}Au foils

S.R. Hashemi-Nezhad [a,*], Igor Zhuk [b], A. Potapenko [b], M. Kievets [b], M.I. Krivopustov [c,1]

[a] Institute of Nuclear Science, School of Physics, University of Sydney, NSW 2006, Australia
[b] Joint Institute of Power and Nuclear Research-Sosny NASB, 220109 Minsk, Belarus
[c] Joint Institute for Nuclear Research, 141980 Dubna, Russian Federation

ARTICLE INFO

Article history:
Received 16 August 2011
Received in revised form
13 October 2011
Accepted 21 October 2011
Available online 7 November 2011

Keywords:
Calibration factor
Fission-rate
Proton-induced fission
Mica detectors

ABSTRACT

Calibration factors *w*, for determination of fission rate in metallic foils of ^{nat}U, ^{235}U, ^{232}Th, ^{nat}Pb and ^{197}Au were determined for foils in contact with synthetic mica track detectors. Proton-induced fission at proton energies of 0.7 GeV and 1.5 GeV were used. Using our experimental results as well as those of the other authors, *w* for different foil–mica systems were determined. Two methods were used to calculate *w*, relative to the calibration factor for uranium–mica system, which has been obtained in a standard neutron field of energy 14.7 MeV. One of these methods requires the knowledge of the mean range of the fission fragments in the foils of interest and other method needs information on the values of the fission cross-sections at the required energies as well as the density of the tracks recorded in the track detectors in contact with the foil surfaces. The obtained *w*-values were compared with Monte Carlo calculations and good agreements were found. It is shown that a calibration factor obtained at low energy neutron induced fissions in uranium isotopes deviates only by less than 10% from those obtained at relativistic proton induced fissions.

1. Introduction

Track detectors provide a valuable technique for determining the fission-rate in fissionable materials in complex particle fields [1]. In order to measure the fission-rate, a calibration factor is required that relates the track density to the number of fission events in the material of interest. Such a calibration factor *w* is dependent on the type of fission–foil and on the type of the dielectric detector registering the tracks. This implies that for each fission–foil-detector system a calibration factor must be obtained.

In an earlier work [2] we have discussed the calibration factor in some detail and have presented experimental and theoretical procedures for its determination. The *w*-values for muscovite mica, synthetic mica (Fluorophlogopite), Lavsan plastic and soda glass detectors in contact with natural and enriched uranium foils are given in reference [2]. In these experiments the fission events were induced by thermal or 14.7 MeV neutrons.

It is shown that the effects of anisotropy in emission direction of fission fragments on the track density, can be eliminated if one uses the mean track density in the detector foils that are in contact with the two faces of a given fission–foil [2].

In this work we present the determination of *w* for synthetic mica in contact with ^{nat}U, ^{235}U, ^{232}Th, ^{nat}Pb and ^{197}Au foils, for relativistic proton induced fission events.

2. Theoretical considerations

The fission rate is related to the track density in a track detector in contact with a fission–foil by the following relationship [2]:

$$\rho = wN_f \tag{1}$$

where ρ is the mean density of tracks in the downstream and upstream detectors (Fig. 1), N_f is number of fissions per atom of fissionable nuclei of the fission–foil during the irradiation time, t, and

$$w = n\mu\varepsilon dN_v \tag{2}$$

is the calibration factor. In Eq. (2) n is the number of fragments per fission event (assumed to be two), d is the thickness of the foil, ε is an efficiency factor, which includes the critical etching angle effect [3] as well as the limitations imposed by the minimum detectable track size at a given track observation conditions [2], N_v is the number of the fissionable nuclei per unit volume of the foil and μ is a parameter that depends on the fission–foil thickness. For the cases in which the foil thickness is larger than

* Corresponding author. Tel.: +61 2 93515964.
E-mail address: reza@physics.usyd.edu.au (S.R. Hashemi-Nezhad).
[1] Deceased

0168-9002/$ - see front matter © 2011 Elsevier B.V. All rights reserved.
doi:10.1016/j.nima.2011.10.029

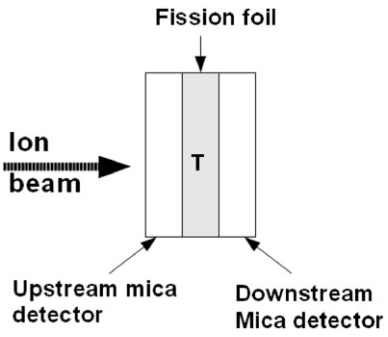

Fig. 1. Schematic drawing of foil-detector assemblies used in experiments and the calculations.

the range of fission fragments R in the foil, μ is given by [2,4]

$$\mu = \frac{1}{4}\frac{R}{d} \tag{3}$$

From Eqs. (2) and (3) we have

$$w = \frac{1}{2}N_v R\varepsilon \tag{4}$$

When the incident particles are mono-energetic, as was the case with our experiments, the fission rate could be expressed as

$$N_f = t\phi(E)\sigma(E) \tag{5}$$

where $\phi(E)$ and $\sigma(E)$ are the flux of the incident particles and fission cross-section at energy E, respectively. From Eqs. (1) and (5) we have

$$\rho = wF(E)\sigma(E) \tag{6}$$

where $F(E)=t\varphi(E)$ is the time integrated fluence of the incident particles.

From Eq. (4) it is evident that the dimension of w is "cm^{-2}". In the present paper and earlier papers [1,2] for dimension of w, "tracks.cm^{-2}.par^{-1}" was used. These two units are equivalent and the latter was obtained from Eqs. (1) and (5), where particle flux and track density are expressed in units of "particles $cm^{-2}\,s^{-1}$" and "tracks cm^{-2}", respectively.

In this work using the following two methods, we determine the calibration factors for the foils of interest relative to a reference foil–mica system for which an accurate calibration factor is known.

Method 1. If the mean ranges of the fission fragments in the foil of interest and the reference foil are known, then using Eq. (4), the calibration factor for the foil of interest relative to a reference foil can be obtained as follows:

$$w_j = w_r \frac{(N_v)_j}{(N_v)_r}\left(\frac{R_j}{R_r}\right)\left(\frac{\varepsilon_j}{\varepsilon_r}\right) \tag{7}$$

where subscripts j and r refer to the foil material of interest and the reference foil, respectively.

Method 2. If both the reference foil and foil of interest were irradiated with the same particle beam and fluence, then using Eq. (6) the calibration factor for foil j is given by

$$w_j = w_r \frac{\rho_j}{\rho_r}\cdot\frac{[\sigma(E)]_r}{[\sigma(E)]_j}. \tag{8}$$

3. Experimental procedure

For every material of interest a sandwich composed of a metallic foil of the fissionable material in close contact with two synthetic mica (Fluorophlogopite) foils, acting as fission track detectors, was prepared as shown in Fig. 1. All foils were considered to be thick; their thickness d was greater than the range of fission fragments in the foil material.

Table 1
Irradiation type for the set of the samples studied in this work. The total proton fluences given in table refer to the total number of the protons contained in the beam and not to those that struck samples.

Foil material	Proton energy (GeV)	Irradiation period	Total beam fluence (protons cm^{-2})	Mean track density (tracks cm^{-2})
^{nat}Pb	0.7	Short	$\sim 2\times10^{11}$	$(1.97\pm0.06)\times10^4$
^{nat}Pb				$(1.99\pm0.06)\times10^4$
^{nat}U				$(1.55\pm0.05)\times10^5$
^{nat}Pb	0.7	Long	1.47×10^{13}	$(4.44\pm0.18)\times10^5$
^{nat}U				$(3.38\pm0.14)\times10^6$
^{nat}Pb	1.5	Short	$\sim 2\times10^{11}$	$(6.10\pm0.18)\times10^4$
^{232}Th				$(3.73\pm0.17)\times10^5$
^{nat}U				$(5.56\pm0.17)\times10^5$
^{235}U				$(6.46\pm0.19)\times10^5$

The prepared sandwiches were irradiated with protons from the Nuclotron accelerator of the Laboratories of High Energy (LHE) at the Joint Institute for Nuclear Research (JINR), Dubna, Russia.

Two irradiations at proton energies of E_p=0.7 GeV and E_p=1.5 GeV were carried out. In each irradiation the sandwiches of different foil materials were all aligned along the same axis, parallel to the proton beam direction; thus, the proton beam was normal to the surfaces of the foils and proton fluence for all foils in a given irradiation was the same. For the 0.7 GeV irradiation foils of ^{nat}U and ^{nat}Pb were used while the 1.5 GeV irradiation included foils of ^{nat}U, ^{235}U (enriched uranium), ^{232}Th and ^{nat}Pb.

For the 0.7 GeV irradiation two irradiation times were used, which in this paper will be referred to as "short" and "long" irradiations. Table 1 gives the irradiation type for the set of the samples studied in this work. The total proton fluences given in Table 1 refer to the total number of the protons contained in the beam and not to those that struck our samples.

After irradiation the mica detectors were etched as described in Ref. [2] and track densities in both mica detectors corresponding to each side of a given foil were measured using an optical microscope. The background track densities in syntactic mica (Fluorophlogopite) were negligible. The uncertainties in the track density measurements for short and the long irradiations were 3% and 4–5%, respectively, depending on the track density in the sample.

For all foils, the track density in the "downstream" detector (Fig. 1) was higher than that in the corresponding "upstream" detector, suggesting the presence of anisotropy in the emission directions of the fission fragments (FF). For each foil, the mean of the track densities in the downstream and upstream detectors was determined (Table 1). In this paper all reported uncertainties refer to one sigma.

4. Registration and detection efficiency

MCNPX 2.7a code [5] was used to calculate the charge and energy distribution of the interaction residues that escape the target foils and enter into mica (Fig. 1). Calculations were made for thick U, Pb and Au target foils when they were irradiated with protons of energy 1 GeV. In this series of calculations the INCL4 intranuclear cascade model [6] and the ABLA evaporation–fission model [7] were used.

In Fig. 2 the left-hand plots show the charge distributions of the ions (fission fragments and spallation residues) that escape the thick targets. The right-hand graphs show the variation of

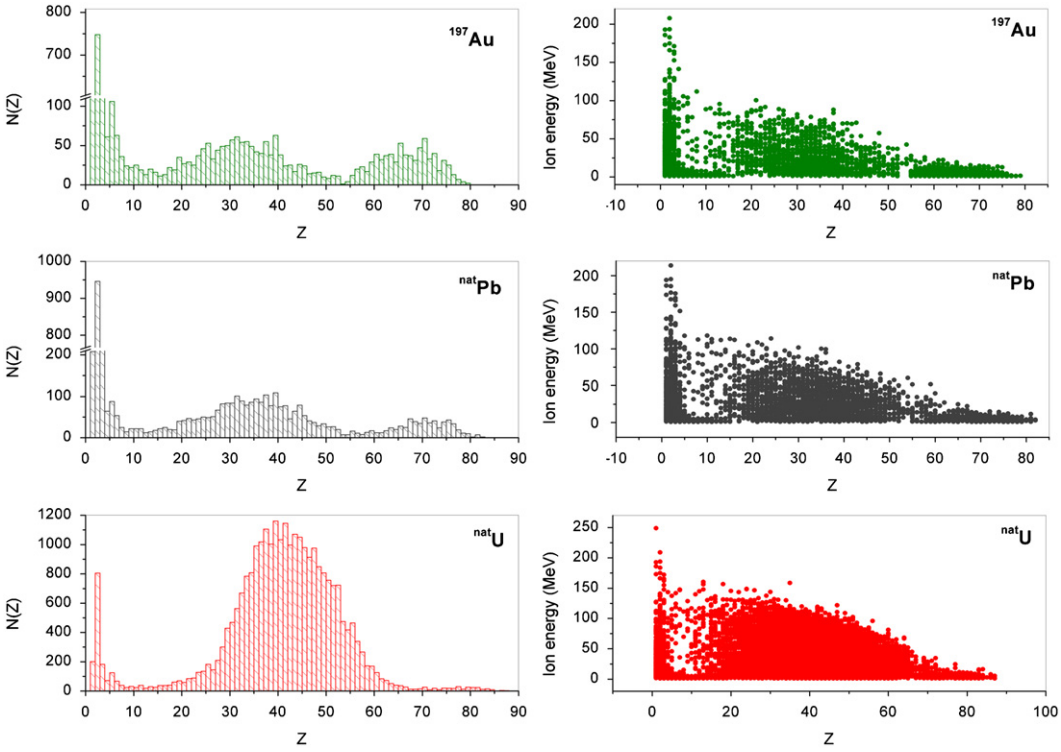

Fig. 2. Left-hand graphs are the charge distributions of the ions (fission fragments and spallation–evaporation residues) that escape the thick target foils (Au, Pb and U) and enter the mica track detectors (Fig. 1). The right-hand graphs show variations of escaping ion energy as a function of ion charge (Z) for different foils. In the calculations, the mica-foil–mica sandwiches (Fig. 1) were irradiated with 1 GeV protons.

escaping ion energy with the charge of the ions, Z for different foils. From Fig. 2, the following observations can be made:

1. In each of the charge distribution plots, the middle peak represents the fission fragments (the fission peak). The peaks on either sides of the fission peak are due to the spallation–evaporation residues.
2. From the charge distribution plots, it is evident that the number of spallation–evaporation residues as compared to fission fragments increases with reducing charge number of the target.
3. In the case of lead and gold targets, the fission fragments occupy a charge range of $\sim$15 to $\sim$55. For uranium target, the fission fragment charge range is $\sim$15 to $\sim$70.
4. By comparing the charge distributions of the residues (left-hand plots) with the plots of the residue ion energies vs Z (right-hand plots), it becomes clear that the high Z spallation–evaporation residues have very low energies and low-Z spallation–evaporation residues have relatively high-energies. The contribution of the spallation–evaporation residues (fragments resulting from the intranuclear cascade and evaporation stages of the interaction) to the measured track densities is negligible and almost all of the registered tracks correspond to the fission events [8].
5. Besides the tracks that originate from interaction of the projectiles with the target (foil) nuclei, there is the possibility of recording tracks that may originate from interactions of the projectile with the constituent nuclei of mica. Fig. 3 shows the charge distribution of fragments produced when a phlogopite mica [$KMg_3(Si_3Al)O_{10}(F,OH)_2$] foil of thickness 1 mm and density 2.83 g.cm^{-3} was irradiated with protons of energy 1500 MeV, as calculated using the MCNPX 2.7a code [5]. Most of these reaction products will not be registered or detected because of the registration and detection limits of the mica as discussed in Ref. [8]. Moreover, measurements of the track density in surfaces of the mica foils that were not facing the target foils showed that track density does not exceed $\sim$150 tracks cm^{-2} (for an ion beam fluence of $\sim 2\times10^{11}$). This is more than two orders of magnitudes less than the tracks density in the mica surfaces that were in contact with the target foils.
6. From the observed charge and energy distributions of the ions it is expected that the registration efficiencies for the fission fragments of the U, Pb and Au would be very similar. In Section 7 of this paper it is shown that such an expectation is not

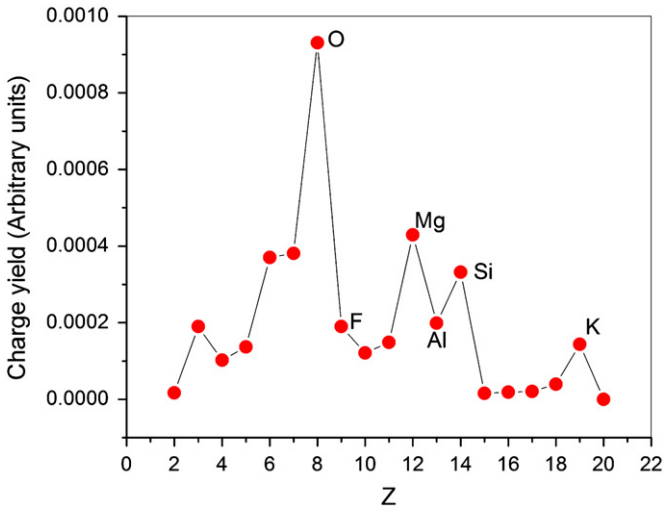

Fig. 3. Calculated charge distribution of fragments produced in the interaction of 1.5 GeV protons with phlogopite mica.

unrealistic. In an earlier work we have obtained a registration-detection efficiency of $\varepsilon=0.77$ for uranium–mica system [2].

5. Results

5.1. Mean range of fission fragments in foil materials

In order to calculate the calibration factor using Eq. (7), one requires the knowledge of the mean range of the fission fragments in the foil materials.

5.1.1. Mean range of uranium fission fragments induced by low energy projectiles in uranium

Here the low energy refers to the incident particle energies at which the spallation is not the main reaction channel. This implies that in interaction of the projectiles with target nuclei, intranuclear cascade and the follow-up evaporations have not taken place. In other words, on average, the charge and mass losses of the target nuclei prior to fission event were not significant.

In earlier work [2] we have given $R_r=5.41$ μm as the mean range of fission fragments in uranium metal for fission induced by relatively low energy neutrons. This mean range has been obtained as $(R_L+R_H)/2$ where R_L and R_H are the ranges of median light and median heavy fission fragments, respectively. R_L and R_H values were obtained using the characteristics of the median fragments as given in Ref. [9]. However more accurate calculations could be made using the procedure described by [10,11]. The mean range was calculated using the following equation:

$$\frac{1}{R_r}\equiv\frac{1}{\langle R\rangle}=\frac{1}{2}\left(\frac{1}{R_L}+\frac{1}{R_H}\right) \tag{9}$$

The obtained mean range $R_r=5.22\pm0.06$ μm is in agreement with the range calculated for the overall average fragment [9], $R_r=5.23\pm0.04$. In calculations of the uncertainties for values of R_r, an uncertainty of 1 MeV is assumed in the kinetic energies of median-light and -heavy and overall average fragments.

5.1.2. Mean range of uranium fission fragments induced by high-energy protons in uranium

We used experimental results on charge, mass and energy distribution of fission fragments produced in ^{238}U+p at 1 A GeV interactions [12], to calculate the weighted mean range of the fragments in metallic uranium for high-energy nucleon induced fission, R_{HE}.

a. Bernas et al. [12] give the mean charge $\langle Z\rangle=44.9\pm0.1$ and standard deviation $\sigma_Z=7.0\pm0.2$ for the charge distribution of the fragments in symmetric fission of ^{238}U+p at 1 A GeV. Using these informations the probability for emission of a fragment with atomic number Z, $P(Z)$, was calculated.
b. Mean kinetic energy of the fragment with atomic number Z, $E(Z)$ was taken from Table 1 of Refs. [12,13] and weighted mean mass of fragment of charge Z, $\langle A_Z\rangle$ was calculated using the mass and cross-section values given in [12,13]. The range of fragment Z in metallic uranium $R(Z)$ was calculated using the SRIM2008 code[14].
c. The weighted mean range of the fragments in uranium was calculated with standard method as

$$\langle R\rangle=\frac{\sum_{Z=28}^{Z=74}P(Z)R(Z)}{\sum_{Z=28}^{Z=74}P(Z)} \tag{10}$$

We obtained $R_{HE}\equiv\langle R\rangle=4.78$ μm.

In the interaction of ^{238}U+p at 1 A GeV, ^{220}Th has been identified as the mean fissioning parent nucleus [12,13]. In this reaction the mean fragment is ^{107}Rh and has a mean kinetic energy of $\langle E_k\rangle=76\pm3$ MeV [12]. Therefore the range of the mean fission fragment in uranium foil in the interaction of ^{238}U with protons at 1 A GeV is $R=4.75\pm0.11$ μm, which is in total agreement with mean range of the fission fragments as value reported above. This agreement suggests that the use of the range of mean fission fragment is a valid method and in doing so, no noticeable error will be introduced in the value of the calibration factor.

5.1.3. Mean range of lead fission fragments induced by high-energy protons in lead

In the case of the lead, two sets of data for ^{208}Pb+p interactions at 1 A GeV [15] and at 0.5 A GeV [16] are available. For interactions at 0.5 A GeV the mean charge $\langle Z\rangle=40.0\pm0.1$, mean mass $\langle A\rangle=93.0\pm0.4$ and total kinetic energy $\langle E_k\rangle=134\pm5$ MeV have been reported [16]. While for the interaction at 1 A GeV, $\langle A\rangle=90.7\pm1.0$, $\langle Z\rangle=39.6\pm0.5$ and $\langle E_k\rangle=64\pm4$ MeV (mean kinetic energy of single fragment) are given in Ref. [15].

Using the data for interactions at 1 A GeV a mean range value of $R=7.84\pm0.31$ μm was calculated. The mean range obtained using the data for interactions at 0.5 A GeV give $R=8.13\pm0.18$ μm. The mean value of these two ranges, $\langle R\rangle=8.06\pm0.35$ μm, will be used as mean-range of the lead fission fragments in lead.

5.1.4. Mean range of gold fission fragments induced by high-energy protons in gold

In the case of gold foil a total fission fragment kinetic energy of 114 ± 2 MeV, mean fragment of mass $\langle A\rangle=84.7\pm0.2$ and mean charge $\langle Z\rangle=37.3\pm0.1$ were used, which have been obtained for ^{197}Au+p interaction at 0.8 A GeV [17]. These data resulted in a mean range of gold fission fragments in gold as $R=4.37\pm0.05$ μm.

It is worth mentioning that changing the type and/or the energy of the incident particle does not noticeably alter the spectrum of the residual ions (fragments) within the foils or the energy release in the fission [8,12].

5.1.5. Mean range of thorium fission fragments induced by high-energy protons in thorium

The experimental work of Guedes et al. [18] shows that the mean etchable length of fission fragments in mica of the thermal neutron induced fission of ^{235}U and fast neutron induced fission of ^{232}Th differ from each other only by 2.5%. If we extend this observation to high energy proton induced fissions then from the mean range of the uranium fission fragments in uranium ($R=4.75\pm0.11$ μm) mean range of the thorium fission fragments in thorium can be calculated using the following equation:

$$R_{Th}=R_U\frac{d_U}{d_{Th}} \tag{11}$$

where d_U and d_{Th} are the densities of the uranium and thorium, respectively. Such calculation results in 7.76 ± 0.18 μm for the mean range of the high-energy proton induced fission fragments in thorium.

5.2. Determination of the calibration factors using mean fission fragment ranges.

Using Eq. (7) and calculated mean range values and assuming $\varepsilon_j=\varepsilon_r$ the calibration factors for high-energy proton induced fission were determined (Table 2). In these calculations the calibration factor for ^{nat}U–mica system $w_r=(9.9\pm0.3)\times10^{18}$ tracks cm^{-2} par^{-1}, which has been obtained in a standard neutron field of 14.7 MeV was used as reference calibration factor [2].

5.3. Determination of the calibration factors using fission cross-sections and track densities

Determination of calibration factors using Eq. (8) requires knowledge of fission cross-sections (for the reference foil and foil of interest) at the energies relevant to the incident particles.

The proton induced fission cross-sections at energies of 0.7 and 1.5 GeV were calculated using the procedures given by Prokofiev [19]. In these calculations, parameters for individual best fits to the available experimental data were used. Table 3 gives the calculated fission cross-sections for the different foil materials used in the experiment.

Using the measured mean track densities (Table 1), fission cross-sections from Table 3 and $w_r \equiv (w_U^{nat})_{HE} = (8.99 \pm 0.22) \times 10^{18}$ tracks cm^{-2} par^{-1} (Table 2), the w_j-values were calculated from Eq. (8) as given in Table 4.

From Table 4 the mean value of the calibration factor for ^{nat}Pb–mica systems at the proton energy of 0.7 GeV is $\langle w_{Pb} \rangle = (1.17 \pm 0.11) \times 10^{19}$ tracks cm^{-2} par^{-1}, which is 28% higher than the value obtained at the proton energy of 1.5 GeV. As the uncertainty in the track density measurements were ~3%, this relatively large discrepancy must be due to the fission cross-section ratio in Eq. (8).

From the values of the w_{Pb} at two energies (0.7 and 1.5 GeV) we obtain a mean value of $\langle w_{Pb} \rangle = (1.10 \pm 0.12) \times 10^{19}$ tracks cm^{-2} par^{-1} for the ^{nat}Pb–mica system.

Table 2
Calibration factors obtained using Eq. (7) for high-energy proton induced fission events.

Foil	Mean FF range (μm)	w_j (tracks cm^{-2} par^{-1})
^{nat}U	4.75 ± 0.11*	(8.99 ± 0.22) × 10^{18}
^{235}U	4.75 ± 0.11*	(9.11 ± 0.22) × 10^{18}
^{232}Th	7.76 ± 0.18	(9.23 ± 0.36) × 10^{18}
^{nat}Pb	8.06 ± 0.35	(1.04 ± 0.05) × 10^{19}
^{197}Au	4.37 ± 0.05	(1.01 ± 0.03) × 10^{19}

* It is assumed that mean ranges of fission fragments of ^{nat}U, ^{238}U and ^{235}U in uranium are the same.

Table 3
Proton induced fission cross-sections from Ref. [19].

E_p (GeV)	Proton induced fission cross-section (mb)			
	^{nat}U	^{235}U	^{232}Th	^{nat}Pb
0.7	1346.6	1383.8	980.0	133.7
1.5	1224.0	1264.4	883.4	132.5

Table 4
Calibration factors obtained using Eq. (8) for high energy proton induced fission events.

Proton energy (GeV)	Irradiation period	Foil type	w_j* tracks cm^{-2} par^{-1}
0.7	Short	^{nat}Pb	(1.15 ± 0.06)E+19
		^{nat}Pb	(1.16 ± 0.06)E+19
	Long	^{nat}Pb	(1.19 ± 0.08)E+19
1.5	Short	^{235}U	(1.02 ± 0.07)E+19
		^{232}Th	(8.46 ± 0.50)E+18
		^{nat}Pb	(9.11 ± 0.45)E+18

* Uncertainties do not include those related to the fission-cross-sections.

6. Monte Carlo calculations

We used Monte Carlo method to calculate the calibration factor w for different foil materials. Calculations were made for mean fission fragment in interaction of high energy protons with the target materials.

In these calculations the method described in Ref. [2] was used:

1) It was assumed that fission events take place in random locations within the volume of a thick foil and mean fission fragment of a given target material represents the overall behaviour of the fragments in the foil and mica detectors.
2) It was assumed that the emission direction of the fission fragments is isotropic. This is not true for high-energy particle induced fissions. However it is shown that the mean of the track densities of the downstream ρ_F and upstream mica foils ρ_B, i.e. $\rho = (\rho_F + \rho_B)/2$, is the same for isotropic and anisotropic emission directions [2] and this mean track density was used in calculation of the w.
3) For mica detector a critical dip angle of $\theta_c = 4.5^\circ$ was used [2], below which the fission fragment tracks cannot be revealed by chemical etching.
4) It was assumed that there is a minimum track size below which the etched tracks will not be identified as tracks (because of the microscope resolution and observational limitations) and therefore are not counted. A track depth limit of $\delta = 1.63$ μm was used [2].
5) The ranges of the fragments in the fission–foil and mica were calculated using the SRIM2008 code [14].

In the interaction of ^{238}U+p at 1 A GeV, ^{220}Th has been identified as the mean fissioning parent nucleus [12,13]. In this reaction, the mean kinetic energy of single fragment is $\langle E_k \rangle = 76 \pm 3$ MeV and mean fragment is ^{107}Rh [12].

In the case of the lead foil, we used $\langle A \rangle = 91$ and $\langle Z \rangle = 40$ as mass and charge of the most probable fission fragment of Pb and $\langle E_k \rangle = 64 \pm 4$ MeV as average kinetic energy of a single fission fragment. These were obtained from the interaction of ^{208}Pb+p at 1 A GeV [15].

In the case of the gold foil a total fission fragment energy 114 ± 2 MeV, mean fragment of mass $\langle A \rangle = 85$ and mean charge of $\langle Z \rangle = 37$ [17] were used. We used the $\langle E_k \rangle = 57 \pm 1$ MeV as the mean kinetic energy of the fragments.

The parameters that were used in the MC calculation of the w_j are summarised in Table 5. The uncertainties in the MC-calibrated calibration factors are due to the uncertainties in the mean kinetic energies of the fragments. The Statistical uncertainties of the calculations were better than 1%.

In the case of the thorium foil mean fission fragment, its energy at high-energy proton induced fission and thus the mean range of fission fragments was not available, so the w_{Th} calculation was based on the data available for 14 MeV neutron induced fission. Such calculation will give a theoretical estimate of the w_{Th}, which is not expected to deviate significantly from that of the

Table 5
Mean charge, mass and fission fragment energy used in the MC calculations.

Target foil	$\langle Z \rangle$	$\langle A \rangle$	$\langle E \rangle$ (MeV)	Ref.
U	45	107	76 ± 3	[12,13]
Pb	40	91	64 ± 4	[15]
Au	37	85	57 ± 1	[17]

high energy proton induced fission similar to the case for the uranium as is shown in the present paper.

1. It was assumed that Ba and Sr represent the median-heavy and median-light fission fragments of thorium, respectively. The median-heavy and -light fission fragment masses were taken from [20] and it was assumed that they represent the above mentioned isotopes.
2. The mean total kinetic energy of 160.39 MeV [21] was used for ^{232}Th fission fragments.

From the MC-calculations a value of $[w_{Th}]_{MC}=8.97\times10^{18}$ tracks cm^{-2} par^{-1} was obtained for a thick thorium-foil in contact with synthetic mica.

In a more detailed MC-simulation the w_{pb} was also calculated using the FLUKA2008 [22,23] and SRIM2008 [14] codes. These calculations consisted of the following steps:

1. Interactions of protons of different energies with a thick lead foil (70 μm) were investigated.
2. For a given proton energy the mass and charge number, energy and direction cosines of each fragment were calculated using the FLUKA2008 code. Fig. 4 shows the mass distribution of residual nuclei in interaction of protons of energy 1.5 GeV with the lead nuclei in the foil. In this figure the shaded area corresponds to the mass distribution of the fragments resulting from high-energy proton induced fission events. Similar calculations were performed for protons with energies 0.7 and 1.0 GeV.
3. An input file containing the information on the fission fragments (as listed above) was constructed for the TRIM code (a part of SRIM code) and the final positions of fission fragments were obtained using this code.
4. The fission track registration efficiency of 77% was used for artificial mica [2].
5. Calibration factor was calculated using the mean values of the tracks in downstream and upstream detectors.

Table 6 gives the w_{Pb}-values obtained using the FLUKA and SRIM codes at three different incident proton energies. The mean value $w_{Pb}=(1.06\pm0.07)\times10^{19}$ tracks Par^{-1} cm^{-2}, which is in total agreement with the w_{Pb}-values obtained with other methods as given in Table 7.

Table 7 gives the values of the w_j obtained using Eqs. (7) and (8) and Monte Carlo methods.

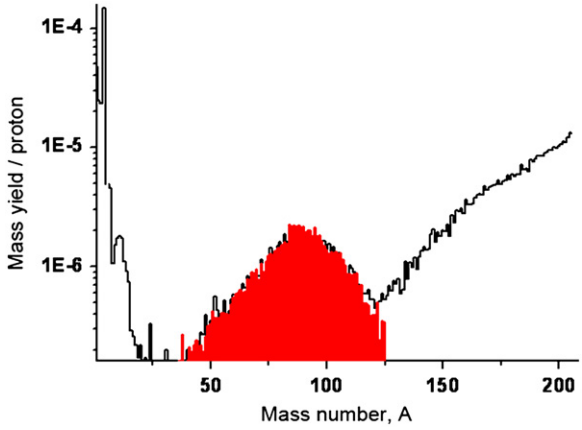

Fig. 4. Mass yield spectrum in interaction of 1.5 GeV protons with lead target as calculated using the FLUKA2008 code.

Table 6
w_{Pb} as obtained using the Fluka2008 and SRIM codes.

Proton energy (GeV)	Calibration factor w (tracks cm^{-2} par^{-1})
0.7	$(1.08\pm0.05)\times10^{19}$
1	$(1.07\pm0.07)\times10^{19}$
1.5	$(1.04\pm0.07)\times10^{19}$

Table 7
Calibration factors obtained using Eqs. (7) and (8) and Monte Carlo method for high-energy proton induced fission events.

Fission foil	Method used for determination of w_j (tracks cm^{-2} par^{-1})		
	Eq. (7)	Eq. (8)	Monte Carlo
^{nat}U	$(8.99\pm0.22)\times10^{18}$	$(8.99\pm0.22)\times10^{18}$*	$(8.51\pm0.32)\times10^{18}$
^{235}U	$(8.99\pm0.22)\times10^{18}$	$(1.02\pm0.07)\times10^{19}$	$(8.51\pm0.32)\times10^{18}$
^{232}Th	$(9.23\pm0.36)\times10^{18}$	$(8.46\pm0.50)\times10^{18}$	$(8.97\pm0.45)\times10^{18}$
^{nat}Pb	$(1.03\pm0.05)\times10^{19}$	$(1.10\pm0.12)\times10^{19}$	$(1.00\pm0.05)\times10^{19}$
^{nat}Pb	–	–	$(1.06\pm0.07)\times10^{19}$**
^{197}Au	$(1.01\pm0.03)\times10^{19}$	–	$(1.01\pm0.01)\times10^{19}$

* This value of w is used as reference calibration factor w_r in the calculations using Eq. (8).
** MC results from FLUKA. Only the statistical uncertainty is taken into account.

7. Discussions and Conclusions

The calibration factor for fission-rate determinations in metallic foils of ^{nat}U, ^{235}U, ^{232}Th, ^{nat}Pb and ^{197}Au were determined for synthetic mica track detector. In this work the calibration factors w_j, were determined relative to w_U whose value has been accurately measured in a standard neutron field of energy 14.7 MeV. The obtained results were compared with those obtained from Monte Carlo calculations. The summary of the obtained results are given in Table 7.

The calibration factors obtained for ^{nat}U, ^{nat}Pb and ^{197}Au, using Eq. (7) (based on the knowledge of the mean range of the fission fragments), Eq. (8) (based on the knowledge of the fission cross-sections and track densities) and Monte Carlo calculations agree within the experimental and statistical uncertainties. They are statistically compatible within 1σ. Such an agreement of the w-values indicate that the assumption of $\varepsilon_j=\varepsilon_r$ was a realistic assumption.

In the case of the ^{235}U sample, w-values from Eqs. (7) and (8) and from Eq. (7) and MC are statistically compatible within 2σ. However the w-values from Eq. (8) and MC agree within 3σ.

The w-value for ^{235}U from Eq. (8) (Table 7), which is based on experimentally measured track densities, is higher than those from Eq. (7) and MC calculations. We believe this is the consequence of fission events in the ^{235}U sample, which were induced by low energy neutrons that were present in the irradiation hall. It should be noted that slow neutron induced fission cross-section of ^{235}U is more than two orders of magnitude higher than that induced by relativistic protons. In this work, the ^{235}U-sample was not shielded against slow neutrons.

In an earlier experiment we have determined w_U^{nat} and w_U^{235} directly using fission induced by 14.7 MeV neutrons as $(9.90\pm0.30)\times10^{18}$ tracks cm^{-2} par^{-1} and $(1.03\pm0.07)\times10^{19}$ tracks cm^{-2} par^{-1}, respectively [2]. These values are larger than w-values for high-energy induced fission events by less than 10%. Such a difference is the direct consequence of the reduction of the mean fission fragments ranges at high-energy particle induced fissions as compared to that at low energy fissions. At high-energy interactions (e.g. 1.0 GeV p+U) charge and mass of the fissioning nuclei are reduced

because of the nucleon losses that takes place in intranuclear cascade and evaporation stages of the interaction prior to the fission. As an example in the interaction of 1.0 GeV p+U the average fissioning nucleus is ^{220}Th with total fission fragment kinetic energy of E_k=152 MeV [12,13] as compared to 14.7 MeV n+^{238}U fission where fissioning nucleus is ^{239}U and $E_k \approx 163$ MeV.

From the above given discussion and the w-values given in Table 7, we reach to the following conclusion:

1. In absence of an accurate value of w, for a fission–foil with $Z \geq 79$ and mica detector, regardless of the energy of the fission inducing particle, using a calibration factor of $w = 1 \times 10^{19}$ (tracks cm^{-2} par^{-1}) will not introduce an uncertainty of more than 10% to the value of the obtained fission rate.
2. As in high-energy interactions, changing the type of the incident particle and its energy, the mean charge, mean mass and mean energy of fission fragments do not change significantly [12]; the above given conclusion applies to different projectile types as well. Moreover, it is shown that increasing the incident proton energy up to 10 GeV does not alter the energy distribution of the reaction residues within the foil [8].

Acknowledgments

SRH would like to thank Australian Institute of Nuclear Science and Engineering (ANSIE) for support of this project under research grant AINGRA09103P.

References

[1] S.R. Hashemi-Nezhad, I. Zhuk, M. Kievets, M.I. Krivopustov, A.N. Sosnin, W. Westmeier, R. Brandt, Nuclear Instruments and Methods in Physics Research Section A: Accelerators, Spectrometers, Detectors and Associated Equipment 591 (2008) 517.
[2] S.R. Hashemi-Nezhad, I. Zhuk, A.S. Potapenko, M.I. Krivopustov, Nuclear Instruments and Methods in Physics Research Section A: Accelerators, Spectrometers, Detectors and Associated Equipment 568 (2006) 816.
[3] R.L. Fleischer, P.B. Price, R.M. Walker, Nuclear Tracks in Solids, University of California Press, 1975.
[4] A.P. Malykhin, O.I. Yaroshevich, V.A. Levadni, L.P. Roginetc, Vestsi AS BSSR, Ser. Phys.-Energ. Navuk 2 (1970) 16.
[5] D.B. Pelowitz, J.S. Hendricks, J.W. Durkee, M.R. James, M.L. Fensin, G.W. McKinney, S.G. Mashnik, and L.S. Waters, MCNPX 2.7.A Extensions, Report LA-UR-08-07182, Los Alamos National Laboratory, November 6, 2008.
[6] A. Boudard, J. Cugnon, S. Leray, C. Volant, Physical Review C 66 (October 2002) 044615.
[7] A.R. Junghans, M. d. Jong, H.-G. Clerc, A.V. Ignatyuk, G.A. Kudyaev, K.-H. Schmidt, Nuclear Physics A 629 (1998) 635.
[8] S.R. Hashemi-Nezhad, I.V. Zhuk, A. Potapenko, M.I. Krivopostov, W. Westmeier, and R. Brandt, Registration of proton induced spallation products of U, Pb and Au in mica track detectors, (2011), Nuclear Instruments and Methods in Physics Research Section A: Accelerators, Spectrometers, Detectors and Associated Equipment. Submitted for publication.
[9] S. Khan, V. Forgue, Physical Review 163 (1967) 290.
[10] F. Rustichelli, Zeitschrift fur Physik 262 (1973) 211.
[11] V. Aiello, G. Maracci, F. Rustichelli, Physical Review B 4 (1971) 3812.
[12] M. Bernas, P. Armbruster, J. Benlliure, A. Boudard, E. Casarejos, S. Czajkowski, T. Enqvist, R. Legrain, S. Leray, B. Mustapha, P. Napolitani, J. Pereira, F. Rejmund, M.-V. Ricciardi, K.-H. Schmidt, C. Stéphan, J. Taieb, L. Tassan-Got, C. Volant, Nuclear Physics A 725 (2003) 213.
[13] M. Bernas, P. Armbruster, J. Benlliure, A. Boudard, E. Casarejos, T. Enqvist, A. Kelic, R. Legrain, S. Leray, J. Pereira, F. Rejmund, M.-V. Ricciardi, K.-H. Schmidt, C. Stéphan, J. Taieb, L. Tassan-Got, C. Volant, Nuclear Physics A 765 (2006) 197.
[14] J.F. Ziegler, J.P. Biersack, U. Littmark, The Stopping and Range of Ions in Matter, Pergamon Press, 1985 See also〈www.SRIM.org〉.
[15] T. Enqvist, W. Wlazlo, P. Armbruster, J. Benlliure, M. Bernas, A. Boudard, S. Czajkowski, R. Legrain, S. Leray, B. Mustapha, M. Pravikoff, F. Rejmund, K.-H. Schmidt, C. Stéphan, J. Taieb, L. Tassan-Got, C. Volant, Nuclear Physics A 686 (2001) 481.
[16] B. Fernández-Domínguez, P. Armbruster, L. Audouin, J. Benlliure, M. Bernas, A. Boudard, E. Casarejos, S. Czajkowski, J.E. Ducret, T. Enqvist, B. Jurado, R. Legrain, S. Leray, B. Mustapha, J. Pereira, M. Pravikoff, F. Rejmund, M.V. Ricciardi, K.-H. Schmidt, C. Stéphan, J. Taieb, L. Tassan-Got, C. Volant, W. Wlazlo, Nuclear Physics A 747 (2005) 227.
[17] J. Benlliure, P. Armbruster, M. Bernas, A. Boudard, J.P. Dufour, T. Enqvist, R. Legrain, S. Leray, B. Mustapha, F. Rejmund, K.-H. Schmidt, C. Stéphan, L. Tassan-Got, C. Volant, Nuclear Physics A 683 (2001) 513.
[18] S. Guedes, R. Jonckheere, P.J. Iunes, J.C. Hadler, Nuclear Instruments and Methods in Physics Research Section B: Beam Interactions with Materials and Atoms 266 (2008) 786.
[19] A.V. Prokofiev, Nuclear Instruments and Methods in Physics Research Section A: Accelerators, Spectrometers, Detectors and Associated Equipment 463 (2001) 557.
[20] In, 〈http://ie.lbl.gov/fission.html〉.
[21] W. Neubert, A.A. Kotov, L.N. Andronenko, A.I. Iljin, G.G. Kovshevny, L.A. Vaishnene, S.S. Volkov, Nuclear Instruments and Methods in Physics Research 204 (1983) 453.
[22] A. Fassò, A. Ferrari, J. Ranft, and P.R. Sala, CERN-2005-10 (2005), INFN/TC_05/11, SLAC-R-773, 2005.
[23] G. Battistoni, S. Muraro, P.R. Sala, F. Cerutti, A. Ferrari, S. Roesler, A. Fassò, and J. Ranft, In: Hadronic Shower Simulation Workshop 2006, (M. Albrow and R. Raja, Eds.), Fermilab 6–8 September, and AIP Conference Proceeding 896, 31–49, (2007).